Kelvin-Helmholtz instability in a strongly coupled dusty plasma medium

Sanat Kumar Tiwari, Amita Das, Dilip Angom, Bhavesh G. Patel, and Predhiman Kaw

Citation: Physics of Plasmas **19**, 073703 (2012); doi: 10.1063/1.4737148
View online: http://dx.doi.org/10.1063/1.4737148
View Table of Contents: http://scitation.aip.org/content/aip/journal/pop/19/7?ver=pdfcov
Published by the AIP Publishing

Kelvin-Helmholtz instability in a strongly coupled dusty plasma medium

Sanat Kumar Tiwari,[1] Amita Das,[1] Dilip Angom,[2] Bhavesh G. Patel,[1] and Predhiman Kaw[1,2]
[1]*Institute for Plasma Research, Bhat, Gandhinagar 382 428, India*
[2]*Physical Research Laboratory, Ahmedabad 380 009, India*

(Received 30 April 2012; accepted 19 June 2012; published online 17 July 2012)

The Kelvin-Helmholtz (KH) instability in the context of strongly coupled dusty plasma medium has been investigated. In particular, the role of transverse shear and the compressional acoustic modes in both the linear and nonlinear regimes of the KH instability has been studied. It is observed that in addition to the conventional nonlocal KH instability, there exists a local instability in the strong coupling case. The interplay of the KH mode with this local instability shows up in the simulations as an interesting phenomenon of recurrence in the nonlinear regime. Thus, a cyclic KH instability process is observed to occur. These cyclic events are associated with bursts of activity in terms of transverse and compressional wave generation in the medium. © *2012 American Institute of Physics*. [http://dx.doi.org/10.1063/1.4737148]

I. INTRODUCTION

Plasma is often found in strongly coupled regime wherein the inter particle potential energy exceeds or is comparable to the kinetic energy of the particle. The coupling parameter $\Gamma = (Ze)^2 exp(-\kappa)/ak_BT \geq 1$ is usually used to demarcate this regime.[1] Here Z is charge on particles, a is inter particle separation (also known as Wigner-Seitz radius), k_BT is the associated kinetic energy of particles under consideration, and κ is the screening parameter providing background plasma shielding effects. Owing to its novel features and its occurrence in a variety of realistic situation, the strongly coupled plasma medium has been a subject of active research both theoretically and experimentally.[2,3] In experiments, the strong coupling regime is achieved by cooling the electron-ion plasma in the electrostatic traps and cyclotrons by means of laser radiation.[4,5] They tend to crystallize and form "Coulomb crystals as well as liquids."[6] Furthermore, the crystallization of electrons at 2D Helium and Hydrogen surfaces are other examples of such a state.[7] While these experiments require fairly complicated apparatus and considerable efforts, it is comparatively easy to produce a dusty plasma medium in strongly coupled state in laboratory. This is because the inter particle separation is small and each of the dust particles can acquire a large number of electrons to be in a highly charged state, e.g. $(10^4 - 10^6)$ electronic charges. A number of microgravity and gravity experiments have shown dust crystallization in the strongly coupled limit.[8–10]

Normally, the coupling parameter Γ remains well below unity for most high temperature plasmas. For instance, for $Z \sim 1$, plasma temperature $\sim 10^6$ K and plasma density as high as $\sim 10^{26}$ cm^{-3}, it turns out that, despite such high density, the plasma lies well within the weakly coupled regime with the coupling parameter below unity. It is thus clearly evident that either high density cold plasma or dusty plasma with very high charge on dust particles can fulfil the condition of $\Gamma \geq 1$.[1] The fact that the dusty plasma could be found in the strongly coupled regime at normal temperatures, it provides a unique test bed and a prime opportunity to investigate the behaviour of a strongly coupled plasma medium over the phase domain ranging from gaseous to solid state.

The weakly coupled dusty plasmas ($\Gamma < 1$) can be easily treated like a fluid. However, in the very strong coupling limit marked by the occurrence of crystallization, it is evident that the fluid model does not adequately describe such plasmas. There is, however, an intermediate regime of the coulomb coupling parameter in which the dusty plasma exhibits properties which are intermediate to fluid and solid like behaviour. This is quite an interesting phase, as the medium behaves like a visco-elastic system.[11] The particles are not rigidly fixed at any locations like in a solid medium. They are free to move around, however, they retain memory of their dynamics. The visco-elastic medium is often described by a generalized hydrodynamic (GHD) model.[12] This model has been successfully adopted earlier by Kaw *et al.* to study the transverse shear waves supported by the strongly coupled dusty plasma medium.[13,14]

The dusty plasma medium often has flows which are sheared, as in case of cometary tails, and protoplanetary disks. In some of these cases, the medium can be in a strongly coupled state. It is well known that shear flows are susceptible to the well known fluid Kelvin-Helmholtz (KH) instability.[15,16] In our recent studies, we had shown the effect of compressibility and dispersion on the KH mode for the dusty plasma medium in the weak coupling regime.[17] The prime aim of the present communication is to investigate KH instability in strongly coupled dusty plasma fluid and in particular to decipher the influence of the transverse shear waves (which are the normal modes of the medium) on the KH instability.

The paper has been organized as follows. Section II provides the details of the governing equations for the visco-elastic dust fluid. In Sec. III, we study the linear regime of the KH instability for such a visco-elastic fluid. We choose a specific tangent hyperbolic form of sheared flow profile for this purpose. The role and effect of strong coupling on the growth rate are discussed and comparison with the weak

coupling limit is provided in this section. We also show the existence of local instability in the strong coupling limit, this is not possible for the normal hydrodynamic fluids. In Sec. IV, we describe the results obtained from the numerical simulation of the GHD model. We show that the growth rate of perturbed energy agrees with the prediction of the linear studies presented in Sec. III. In the nonlinear regime, the simulations show fascinating features. A phenomenon of the recurrence of the KH instability is seen due to the repeated sharpening of the shear width of flow. In addition, these cyclic events are associated with a burst of activity in terms of the emission of transverse and compressional waves. In Sec. V, we summarize our observations.

II. GOVERNING EQUATIONS

We provide here the equations governing the dust fluid dynamics in the presence of effects due to strong coupling. The evolution of dust density is governed by the continuity equation

$$\frac{\partial n}{\partial t} + \nabla \cdot (n\vec{v}) = 0. \tag{1}$$

The momentum equation has the generalized form to incorporate the visco-elastic effects

$$\left[1 + \tau_m \left(\frac{\partial}{\partial t} + \vec{v} \cdot \nabla\right)\right] \left[\left(\frac{\partial}{\partial t} + \vec{v} \cdot \nabla\right)\vec{v} + \frac{\nabla P}{n} - \nabla\phi\right] = \eta \nabla^2 \vec{v}. \tag{2}$$

Here $\vec{v}$ is the dust velocity. The memory effect related to elasticity is incorporated through a relaxation time parameter τ_m, and η is the viscosity coefficient. If $\tau_m d/dt < 1$, then the dust fluid is in the weak coupling regime. While if $\tau_m d/dt \geq 1$, the time scale for which the dust fluid retains its memory is much longer than the phenomenon under consideration. This is the usual description of the visco-elastic fluid through the GHD model.[18] However, the dusty plasma being a charged system, an additional force representing the external/self consistent electric field has to be incorporated. The term $\nabla\phi$ with ϕ representing the scalar potential, takes care of this. The Poisson's equation is used to obtain ϕ self consistently

$$\nabla^2 \phi = n + \mu_e \, exp\,(\sigma_i \phi) - \mu_i \, exp\,(-\phi). \tag{3}$$

The time scales associated with the evolution of the heavier dust species being considerably slow compared to ions and electrons, these lighter species are assumed to respond instantaneously and hence their density is given by the Boltzmann distribution

$$\begin{aligned} n_e &= \mu_e \, exp\,(\sigma_i \phi), \\ n_i &= \mu_i \, exp\,(-\phi), \end{aligned} \tag{4}$$

Here $\sigma_i = \frac{T_i}{T_e}$ denotes the ratio of ion to electron temperature, $\mu_e = \frac{n_{e0}}{Z_d n_{dN}}$, and $\mu_i = \frac{n_{i0}}{Z_d n_{dN}}$, where n_{dN} is the normalizing density for the dust fluid and Z_d is the negative charge on each dust particle. The equilibrium densities have been denoted by the subscript 0 and they satisfy the quasineutrality condition $n_{i0} = Z_d n_{d0} + n_{e0}$ for dusty plasmas. The normalized number densities for dust, ion, and electron species are $\bar{n} = \frac{n_d}{n_{dN}}$, $\bar{n}_i = \frac{n_i}{n_{iN}}$, and $\bar{n}_e = \frac{n_e}{n_{eN}}$, respectively. Here, n_{sN} $(s = e,i,d)$ denote the normalizations of the number density of the specific species. Time and length are normalized by ω_{pd}^{-1} and λ_D, respectively, with $\omega_{pd} = \left(\frac{4\pi (Z_d e)^2 n_{d0}}{M_d}\right)^{1/2}$ (M_d is mass of dust particle) being the dust plasma frequency and $\lambda_D = \frac{k_B T_i}{4\pi n_{dN} (Z_d e)^2}$. The normalized scalar potential is $\bar{\phi} = \frac{Z_d e \phi}{k_B T_i}$. The pressure is determined using equation of state $P = \mu_d \gamma_d n k_B T_d$. Here $\mu_d = \frac{1}{T_d} \frac{\partial P}{\partial n_d}|_T$ is compressibility parameter and γ_d is adiabatic index. The parameters μ_d, τ_m, and η are empirically related to each other. The empirical relationship is obtained by the Molecular Dynamic simulations.[19,20] Experimentally τ_m, the relaxation parameter can be calculated with estimation of the phase shift between the stress and the shear rate in oscillatory tests.[21] We have chosen a simplified geometry, where variations are confined in 2D x–y plane and the third dimension of $\hat{z}$ is the axis of symmetry. The equilibrium flow is assumed to be directed along y and sheared along x. Thus, the flow direction (i.e., y) is assumed periodic at the boundary while the shear direction (i.e., x) is considered to be nonperiodic at the boundary. For the purpose of our investigation, we take the basic equilibrium flow to have the following form:

$$\vec{v_0} = v_{y0}(x)\hat{y}. \tag{5}$$

In Sec. III, we study the stability of this flow in the 2D x–y plane, wherein the role of strong coupling effects would be investigated.

III. LINEAR STUDIES

We linearize Eqs. (1)–(3) in the presence of the equilibrium flow defined by Eq. (5). The field variables are perturbed such that

$$\vec{v} = v_{1x}\hat{x} + [v_{y0}(x) + v_{1y}]\hat{y}; \quad n = n_0 + n_1; \quad \phi = \phi_1. \tag{6}$$

Here the fields with subscript "1" denote the perturbed fields and those with subscript "0" represent the equilibrium. The linearized equations upon Fourier analysing in time and the y coordinate yields the following:

$$\begin{aligned} &-i\Omega n_1 + n_0 v_{1x}' + i k_y n_0 v_{1y} = 0, \\ &(1 - i\tau_m \Omega)(-i\Omega v_{1x} + \alpha n_1' - \phi') = \eta (v_{1x}'' - k_y^2 v_{1x}), \\ &(1 - i\tau_m \Omega)(-i\Omega v_{1y} + v_{1x} v_0' + i k_y \alpha n_1 - i k_y \phi_1) = \eta (v_{1y}'' - k_y^2 v_{1y}), \\ &\phi_1'' - k_y^2 \phi_1 = n_1 + (\mu_e \sigma_i + \mu_i)\phi_1. \end{aligned} \tag{7}$$

Here $\Omega = \omega - k_y v_{y0}$, the superscript $'$ shows the derivative with respect to x and $\alpha = \mu_d \gamma_d T_d / T_i Z_d$. The parameter $\sqrt{\alpha}/V_0$ in such a case represents the ratio of sound speed with dust flow velocity and hence is typically the inverse Mach number of the dusty plasma flow under consideration. Here V_0 is the amplitude of initial sheared flow velocity. Thus by choosing the value of α ranging from $0 - \infty$ one

can carry out investigation for an incompressible dusty plasma medium to a compressible case. The system of equations gets simplified if we concentrate only on long wavelength quasineutral responses. In view of this, the left hand side of the Poisson's equation can also be ignored. This assumption is followed in both Subsections III A and III B. The assumption of incompressibility simplifies the system of equations even further, as one can then choose $\nabla \cdot \vec{v} = 0$ and neglect the continuity equation. We discuss this particular simplified incompressible limit in the Subsection III A. The general case is then discussed in the subsequent Subsections III A and III B.

A. Incompressible dust fluid

The incompressibility assumption simplifies the set of linearized equations (7) wherein they can be represented in terms of v_{1x} alone

$$k_y\Omega(1-i\tau_m\Omega)^2 v_{1x} - \left(v_{1x}v''_{y0} + \frac{\Omega v''_{1x}}{k_y}\right)(1-i\tau_m\Omega)^2 + \frac{i\eta}{k_y}(v''''_{1x} - k_y^2 v''_{1x})(1-i\tau_m\Omega) + \eta\tau_m v'_{y0}(v'''_{1x} - k_y^2 v'_{1x}) = i\eta k_y(v''_{1x} - k_y^2 v_{1x})(1-i\tau_m\Omega). \quad (8)$$

Rearranging the above equation we can write Eq. (8) alternatively as

$$v''''_{1x} - \frac{ik_y\tau_m v'_{y0}}{(1-i\tau_m\Omega)}v'''_{1x} - 2k_y^2 v''_{1x} + \frac{ik_y^3\tau_m v'_{y0}}{(1-i\tau_m\Omega)}v'_{1x} + k_y^4 v_{1x} - \frac{ik_y^2\Omega(1-i\tau_m\Omega)}{\eta}v_{1x} + \frac{ik_y(1-i\tau_m\Omega)}{\eta}\left(v_{1x}v''_{y0} + \frac{\Omega v''_{1x}}{k_y}\right) = 0. \quad (9)$$

In the incompressible case, the fluid velocity can be expressed in terms of a stream function so as to have $v_{1x} = \partial\Psi/\partial y$ and $v_{1y} = -\partial\Psi/\partial x$, Eq. (9) then can be written in terms of stream function Ψ as

$$\left[\frac{d^2}{dx^2} - k_y^2\right]^2\Psi = \frac{ik_y(1-i\tau_m\Omega)}{\eta}\left[\frac{-\Omega}{k_y}\left(\frac{d^2}{dx^2} - k_y^2\right) - \frac{d^2 v_{y0}}{dx^2}\right]\Psi + \frac{ik_y\tau_m dv_{y0}/dx}{(1-i\tau_m\Omega)}\left[\frac{d^3}{dx^3} - k_y^2\frac{d}{dx}\right]\Psi. \quad (10)$$

It can be easily seen that Eq. (10), in the limit of $\tau_m = 0$, reduces to the linearized equations discussed by Drazin for the KH mode in viscous fluids.[15]

Seeking strong coupling effects on the instability driven by the shear flow, we choose the limit of $\omega\tau_m \gg 1$. In this case Eq. (9) reduces to

$$v''''_{1x} + \frac{k_y v'_{y0}}{\Omega}v'''_{1x} - \left(2k_y^2 - \frac{\Omega^2\tau_m}{\eta}\right)v''_{1x} - \frac{k_y^3 v'_{y0}v'_{1x}}{\Omega} + \left(k_y^4 + \frac{k_y\tau_m\Omega v''_{y0}}{\eta} - \frac{\Omega^2\tau_m k_y^2}{\eta}\right)v_{1x} = 0. \quad (11)$$

In the absence of equilibrium flow, one clearly obtains the dispersion relation of the pure transverse shear wave from Eq. (11)

$$\frac{\omega^2}{k^2} = \frac{\eta}{\tau_m}.$$

We next consider the local limit, wherein the equilibrium velocity flow is assumed to vary rather slowly in comparison to the perturbation scales. In this limit v_{y0} and its derivative can be treated as parameters in a local sense. The system can then be Fourier analyzed in the x coordinate as well. This yields

$$\Omega^3 - \frac{k_y}{|k|^2}v''_{y0}\Omega^2 - \frac{\eta}{\tau_m}|k|^2\Omega + i\frac{\eta}{\tau_m}k_x k_y v'_{y0} = 0. \quad (12)$$

Equation (12) is a cubic equation in Ω and reduces to a quadratic form for the case when $v'_{y0} = 0$ but the second derivative term v''_{y0} is taken as finite. In can be shown that in this case we get a stable system as

$$\Omega = \left(\frac{1}{2}\right)\left[\frac{k_y v''_{y0}}{|k|^2} \pm \sqrt{\left(\frac{k_y^2 {v'_{y0}}^2}{|k|^4} + \frac{4\eta|k|^2}{\tau_m}\right)}\right].$$

However, we observe that the presence of finite v'_{y0} can result in producing a local instability for the system. This has been illustrated by the plots of Fig. 1 which shows a finite imaginary positive value of ω for various set of parameters. Such a local instability is altogether absent in the case of sheared flows in neutral hydrodynamic fluids. Thus, this is one of the new features associated with strong coupling properties of the system. Furthermore, it can also be seen that the transverse shear waves acquires a weak dispersion in the presence of v'_{y0}.

B. The general case

The Eigen values of the complete general set of linearized Eq. (7) can be obtained numerically for specific choices

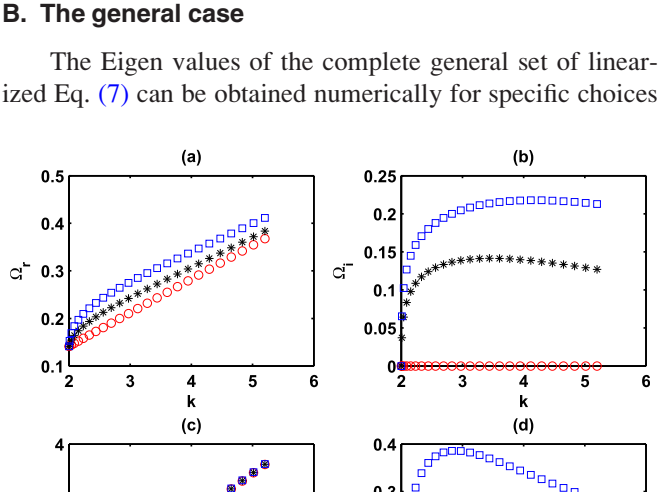

FIG. 1. Dispersion relation for Eq. (12) with finite v'_{y0} parameter while other parameters are $\eta = 0.1, \tau_m = 20$ for subplot (a) and (b) and $\eta = 10, \tau_m = 20$ for subplot (c) and (d). v''_{y0} is taken to be zero. For all subplots, v'_{y0} is 0, 0.4, and 0.8 represented by circle, star, and square, respectively.

of the flow profile. The set of equations involves four fields and it takes considerable time to find the Eigen spectrum and the parameter scan for the study of the influence of strong coupling effects. As an alternative, one can employ a simplified case of quasineutral response for which the dispersive effects appearing in Poisson equation could be ignored. This leads to a simple algebraic relationship between the potential and the density perturbations

$$\phi_1 = -n_1/(\mu_e\sigma_i + \mu_i). \tag{13}$$

We have shown in our earlier studies on weakly coupled dusty plasma system that dispersive effects reduce the growth rate, however, the reduction is insignificant at high values of the α parameter. We therefore prefer to consider the quasineutral case, defined by the following simplified equation

$$\begin{aligned} &-i\Omega n_1 + n_0 v'_{1x} + ik_y n_0 v_{y1} = 0,\\ &(1 - i\tau_m\Omega)(-i\Omega v_{1x} + \alpha_1 n'_1) = \eta(v''_{1x} - k_y^2 v_{1x}),\\ &(1 - i\tau_m\Omega)(-i\Omega v_{1y} + v_{1x}v'_0 + ik_y\alpha_1 n_1) = \eta(v''_{1y} - k_y^2 v_{1y}), \end{aligned} \tag{14}$$

to study the effects of strong coupling. Here $\alpha_1 = \alpha/n_0 + 1/(\mu_e\sigma_i + \mu_i)$. In present case, the Tangent Hyperbolic function is used to represent the equilibrium flow profile and its form is given as

$$\vec{v}_0 = V_0 \tanh\left(\frac{x}{\epsilon}\right)\hat{y}. \tag{15}$$

The set of Eqs. (14) is discretize in x direction and Eigenvalues ω are obtained numerically. The positive imaginary part of Eigenvalues provides the growth rate γ.

The influence of the strong coupling parameters, η and τ_m, on the growth rate of the KH mode is evident from Figures 2 and 3. Here, γ/V_0 is plotted as function of $k_y\epsilon$ for

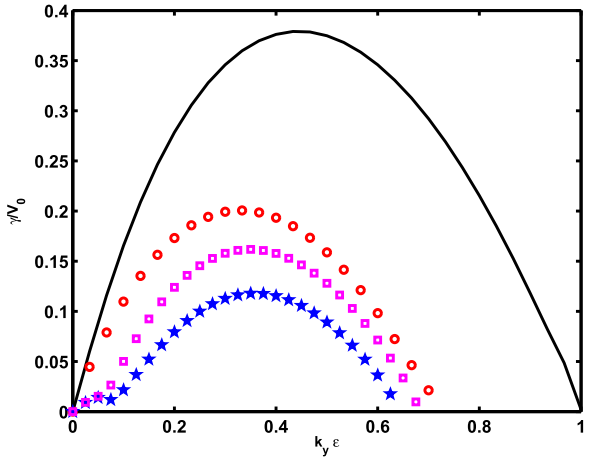

FIG. 2. The scaled growth rate γ/V_0 vs $k_y\epsilon$. The smooth line (black) represents the scaled growth rate of incompressible dust fluid and rest all are compressible cases with Mach No. 0.707 with circles (red) for weakly coupled dust fluid while square (magenta) and stars (blue) represents case of $\eta = 2$ and $\eta = 5$, respectively, for strongly coupled dust fluid. The value of τ_m is kept fix at 20 for these strong coupling cases. The other parameters are $V_0 = 5$ and $\epsilon = 0.5$ (shear width as defined in Eq. (15)).

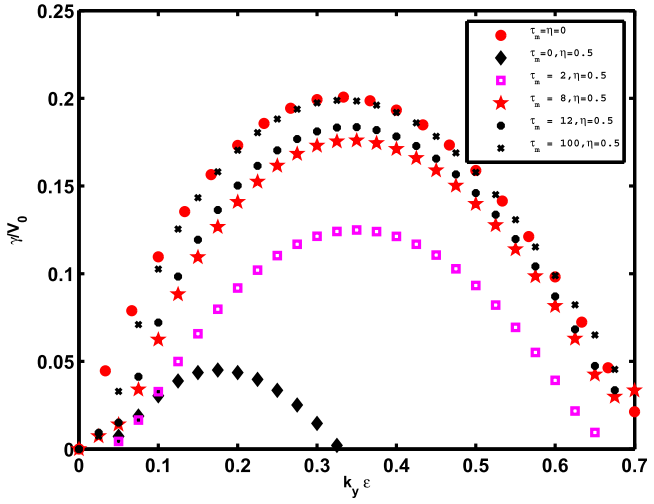

FIG. 3. The scaled growth rate γ/V_0 vs $k_y\epsilon$ for fixed value of $\eta = 0.5$ and various values of $\tau_m = 0$ (diamond), $\tau_m = 2$ (square), $\tau_m = 8$ (star), $\tau_m = 12$ (dot), and $\tau_m = 100$ ($\times$ mark). The red circles show the case of weakly coupled dust fluid. The other common parameters are $V_0 = 5$, $\epsilon = 0.5$ and mach No. 0.707.

various cases. In Figure 2, the growth rate curve for the incompressible weakly coupled dusty plasma system (the hydrodynamics case) has been shown by a black thick line for the reference. For the rest of the plots, the value of Mach number has been chosen to be 0.707, and hence they all have effects due to compressibility. The plot with circles (with red color online) is again for a weakly coupled dust fluid. For this Mach number of 0.707, when the value of η parameter is increased (keeping τ_m fixed), the growth rate is found to decrease and the threshold wavenumber for instability also reduces. The variation in growth rate with respect to τ_m has another interesting aspect. We observe that the growth rate curves for strongly coupled compressible flows (with a given Mach number) are bounded between two curves for a given value of the viscosity parameter $\eta = \eta_s$. The upper and lower bounds correspond to the growth rate of the weakly coupled fluid $\tau_m = 0$, inviscid ($\eta = 0$) and viscous (with viscosity parameter $\eta = \eta_s$) cases, respectively. The upper bound growth rate curve corresponds to $\eta = 0$ and $\tau_m = 0$, is shown by red circles in Fig. 3 and the lower bound growth rate curve corresponds to $\eta = \eta_s$ and $\tau_m = 0$, is shown by diamonds in Fig. 3.

As τ_m is increased for all cases of $\eta = \eta_s$, the growth rate increases from the lower curve and merges with the upper curve at very high values of τ_m. Similar observations were made in our earlier studies on simulations of 1D dusty plasma systems[18] where the strongly coupled dust behaviour described by the GHD set of equations, at very high values of τ_m behaved similar to an inviscid weakly coupled hydrodynamic dust fluid.

It appears that in the limit of $\tau_m \to \infty$ the unity from the operator $1 + \tau_m d/dt$ [Eq. (2)] can be ignored. Dividing the equation by τ_m, one can then ignore $\eta/\tau_m\nabla^2\vec{v}$ from right hand side. Thus, one is left with an equation which has the form of the weakly coupled fluid system with an additional time derivative acting on all the terms.

IV. NONLINEAR STUDIES

We have also investigated the nonlinear regime of the instability numerically, for which, the complete set of equations defined by Eqs. (1)–(3), were utilized. The quasineutral assumption is considered for these numerical studies. The assumption of incompressibility has not been invoked *a priori* for any of the cases studied in simulations. A flux corrected scheme proposed by Boris *et al.*,[22] was used to evolve Eqs. (1), and (2) in the 2D *x-y* plane. As the scheme numerically solves the continuity form of equations with possibility of inclusion of various source terms, we split Eq. (2) as two separate equations of the following form:

$$\left[1+\tau_m\left(\frac{\partial}{\partial t}+\vec{v}\cdot\nabla\right)\right]\vec{\psi}=\eta\nabla^2\vec{v},$$
$$\left(\frac{\partial}{\partial t}+\vec{v}\cdot\nabla\right)\vec{v}+\alpha\frac{\nabla n}{n}-\nabla\phi=\vec{\psi}. \tag{16}$$

The initial condition is chosen as

$$v_x=v_{1x}=V_1k_{yp}\cos(k_{yp}y)\exp(-x^2/\sigma^2),$$
$$v_y=v_{1y}=V_0\tanh\left(\frac{x}{\epsilon}\right)+V_1\left(\frac{2x}{\sigma^2}\right)\sin(k_{yp}y)\exp(-x^2/\sigma^2). \tag{17}$$

The first term in the expression for v_y represents the equilibrium flow of Tangent hyperbolic profile defined in Eq. (15) and the second term represents the perturbation added to the equilibrium flow. Here k_{yp} is the perturbation mode which has been excited to facilitate the growth of instability. The form of the perturbed velocity is so that its effects die out in nonperiodic direction before hitting the boundary of simulation box. The value of parameters chosen in a typical run are $V_0=5.0, V_1=10^{-2}, \sigma=0.8$, and $\epsilon=0.5$. The evolution is tracked by studying the evolution of the total perturbed kinetic energy, $E_{PKE}=\int\int|(\vec{v}-\vec{v}_0)|^2dxdy$. The spatial profiles of velocity, density and potential obtained from simulation were also stored at regular intervals. The evolution of the E_{PKE} for one typical simulation case has been shown in the plot of Figure 4. It is evident that during the initial phase the linear instability mechanism is operative. The growth rate obtained from simulations is observed to match well with the predictions of the linear analysis. In the nonlinear regime, the behaviour of the E_{PKE} evolution in the strongly coupled case differs from what is seen in the other weakly coupled fluid cases. For instance, the simulations of incompressible fluid shows saturation and a constancy of E_{PKE} and the compressible and the dispersive cases show periodic oscillations in E_{PKE} (Ref. 17) in the nonlinear regime. These periodic oscillations are attributed to the rotation of the vortex structure that is ultimately formed as a result of the KH instability. In case of incompressible fluid, the final saturated structure typically has a circular form and its rotation does not cause any periodic changes in E_{PKE}. However, for the compressible and dispersive cases, the vortices that finally form have an elliptical shape. Their rotation then shows up as periodic oscillations in the E_{PKE}. The rotation frequency of the vortex closely matched with the

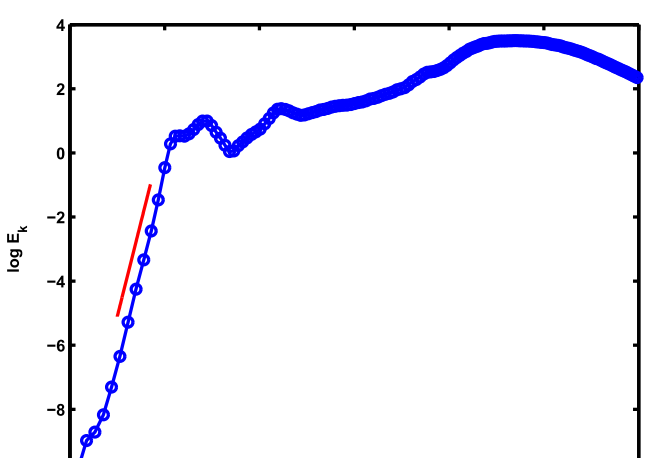

FIG. 4. The Perturbed kinetic energy (log scale) Vs. time for the strong coupling dust fluid. $\eta=5$ and $\tau_m=20$ has been chosen for this case. Other parameters in simulation are same as Fig. 2.

observed oscillation in E_{PKE} in these cases. It was also observed that when the vortices merge an irreversible sudden increase in the value of E_{PKE} is observed. In the strong coupling case, even though the E_{PKE} did exhibit non-stationarity in nonlinear regime, no corresponding periodic characteristics could be identified. We would see later that this absence of oscillatory nature is associated with the elasticity of the medium causing the sharpening of the shear layer and recurrence of the KH excitation phenomena for a couple of times.

We show in Figures 5 and 6 the snapshots of the 2D spatial profile of the curl and the divergence of the velocity field, respectively, for the simulation run corresponding to plot of E_{PKE} evolution shown in Figure 4. The initial state is chosen divergenceless ($\nabla\cdot\vec{v}=0$) and constitutes uniform strip of vorticity. During the linear phase $t=10.01$ (comparison of timing can be seen from Fig. 4), the usual bending of the vorticity strip due to the KH instability can be seen. At later stage, it breaks up into anisotropic vorticity patches. Apart from the vorticity patches at the main central region, the emission of transverse waves separating from the central region and moving towards the boundaries can also be discerned clearly from the snapshots. These emissions are caused by the local instability which is possible in the case of the strongly coupled medium and about which we discussed in Sec. III earlier. The spatial profile of divergence shown in Fig. 6 illustrates the compressional nature of these emissions.

These vorticity patches, however, are observed to change their shape as they rotate. This is quite unlike the other cases (e.g., incompressible and compressible weakly coupled fluids). Here, the vorticity patches get stretched against the background flow, as they rotate. The elastic nature of the medium in this case lets the vorticity patch get extended. The extended structures then coalesce again to form a very thin vorticity strip (see blue colored patches in online publication) as shown in the snapshots of Fig. 5 at $t=18.69$ and $t=19.62$). During this extension and coalescence phase, there is an intense activity in terms of the emission of shear waves. This is reminiscent of the process when

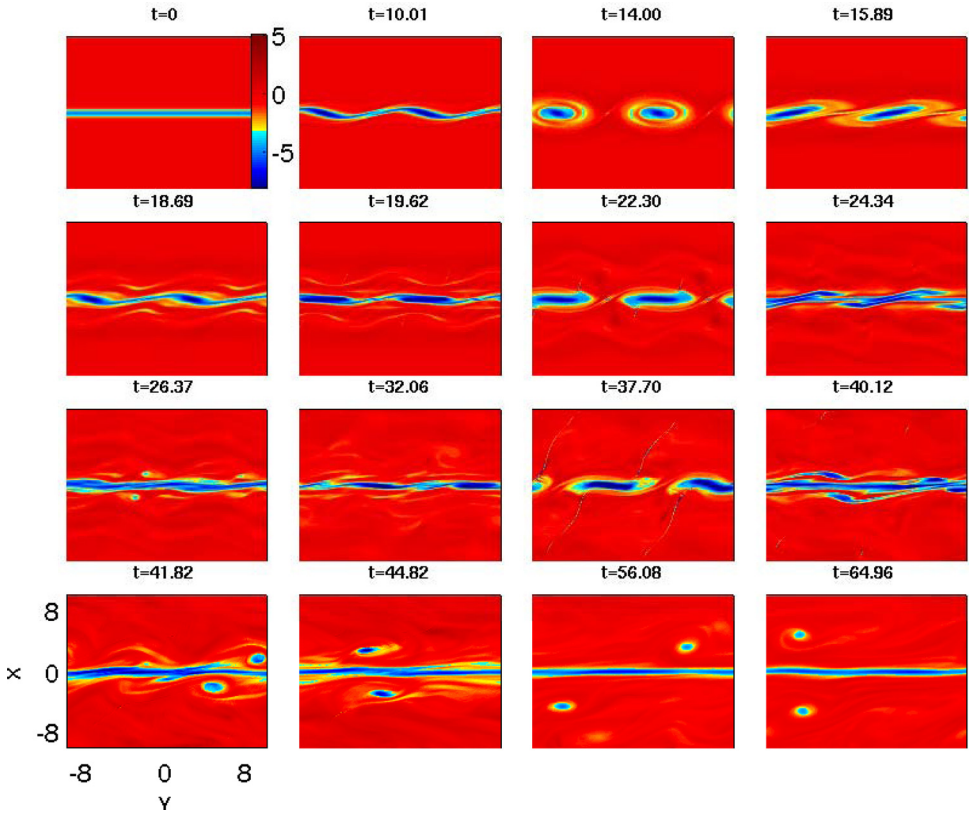

FIG. 5. Nonlinear evolution of vorticity contours at different times for parameter values $\eta = 5, \tau_m = 20$ and mach No. 0.707 for this case. Other simulation parameters are $V_0 = 5$ and $\epsilon = 0.5$. Quasi-neutrality has been taken under consideration.

an elastic medium as it snaps back produces intense oscillations. It is interesting to observe that the thin central vorticity strip developed after the coalescence is now again sharp enough to suffer KH destabilization. This again results in the formation of rotating vortices ($t = 22.30$). The same process then repeats itself. At a later stage one, also observed that smaller lumps of vorticity gets separated from the central region. This is as if the medium yields and breaks apart, as it is no longer possible for it to sustain the strain. Some of these smaller structures upon reaching the region of uniform background flow form circular patterns and are seen to be well preserved for quite a long duration.

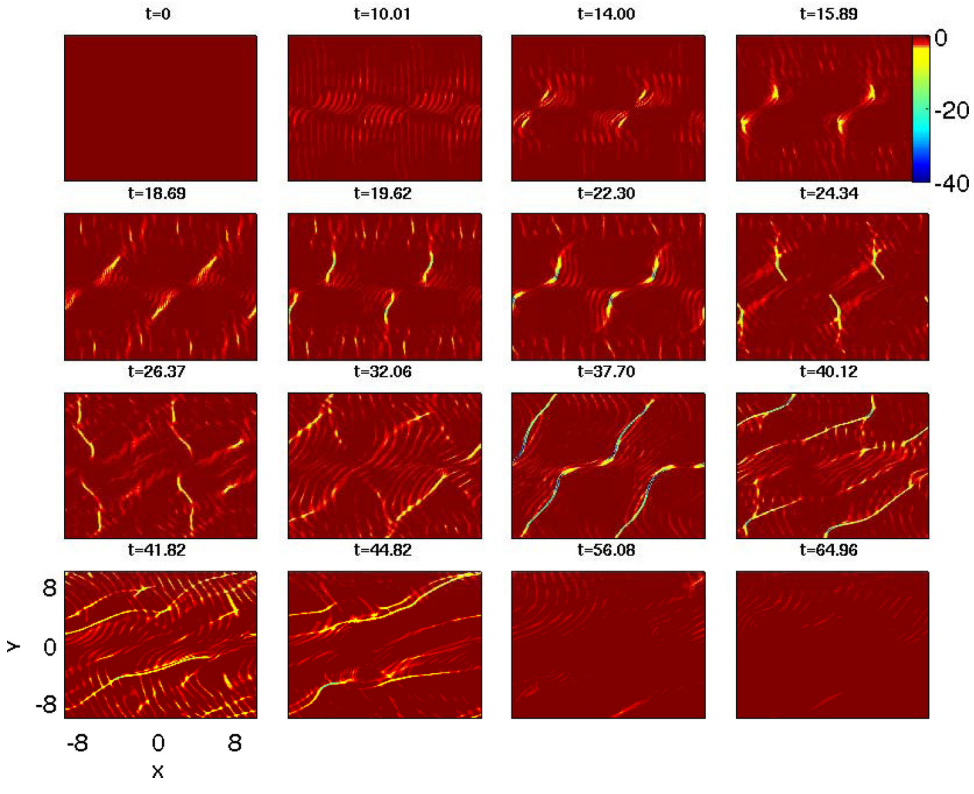

FIG. 6. Nonlinear evolution of divergence of velocity field contours at different times for parameter values $\eta = 5, \tau_m = 20$ and mach No. 0.707 for this case. Other parameters in simulation are $V_0 = 5$ and $\epsilon = 0.5$. Quasineutrality has been taken under consideration.

This entire repetitive nature of the process can be summarized as follows:

- *Initial configuration*: Initially, the shear scale $\epsilon = \epsilon_{init}$ is sharp enough to cause destabilization of shear flow (Fig. 5, subplot at $t = 0$ and $t = 10.01$).
- *Nonlinear regime*: In this regime, the effective shear width ($\epsilon = \epsilon_{eff}$) is broader and the growth of KH mode is no longer sustained. The saturated KH mode forms elliptical vortices (Fig. 5, subplots at $t = 14.00$, $t = 22.30$, and 37.70).
- *Elliptical vortices*: The elliptical vortices formed in nonlinear regime rotate and get stretched by the background flow. Basically, the elastic nature of the medium stretches the elliptical vortices further to form sharp shear flow structures (Fig. 5, subplots at $t = 15.89$, $t = 24.34$, and $t = 40.12$).
- *Coalescence of sharper elliptical vortices*: Elongation of elliptical vortices leads to formation of a sharper shear width and hence this configuration is once again susceptible to KH destabilization (Fig. 5, subplots at $t = 18.69$ and $t = 26.37$).
- *Recurrence*: Thus, the phenomena of KH destabilization recur in this case of strong coupling. (Fig. 5, subplots at $t = 19.62$ and $t = 32.06$).

V. SUMMARY

The fluid Kelvin-Helmholtz instability in the context of a strongly coupled dusty plasma medium has been investigated in detail. In particular it is of interest to understand the role of visco-elasticity and the existence of transverse shear waves in a strongly coupled medium on the fluid KH instability. A generalized fluid hydrodynamic model (GHD), which captures these aspects of the strong coupling state, has been used to represent the behaviour of dusty plasma medium in this regime.

A complete parametrization of the KH growth rate, in terms of the memory relaxation parameter employed in the GHD model to depict strong coupling effect, has been carried out. It is observed that the growth rate of KH mode reduces in a strongly coupled medium. Furthermore, in addition to the KH mode, a local instability driven by the shear flow is also found to exist in the strongly coupled medium. The existence of this local mode causes emission of transverse shear modes. These linear results were verified in the nonlinear simulations conducted by us.

The simulations showed interesting phenomena of recurrence of the KH mode in the nonlinear regime. The KH mode typically saturates by generating vorticity structures which typically have much broader width for sustaining the KH mode. The 2D constraints of the normal fluid on enstrophy can only make the scale lengths associated with the shear scale get further broadened due to coalescence in the case of normal fluids. However, the GHD fluid has no such constraint in 2D. In fact, the elastic nature of the strongly coupled fluid causes the individual vortices as they rotate to get stretched and form sharper flow structures. Thus, unlike a 2D normal fluid in a 2D visco-elastic fluid one observes formation of short scale structures. These sharp structures are then again susceptible to the KH instability. This cycle was observed to get repeated several times in some of our simulations. It ultimately stops as a result of system exhausting up its free energy associated with the shear flows. An additional channel of free energy exhaustion associated with shear flow, is the local instability supported by the medium due to which strong emission of transverse as well as compressional waves are observed. We have demonstrated a rich variety of response in a 2D strongly coupled visco-elastic dusty plasma medium by our simulations conducted here for an equilibrium shear flow configuration. Further studies to understand the competition between the local instability and the KH mode in getting rid of the free energy associated with the shear flow in a visco-elastic medium is necessary. It is also clear from our simulations that in a 2D visco-elastic medium the possibility of formation of short scales does exist. Thus, unlike the hydrodynamic fluid the cascade behaviour of the spectrum is quite distinct and should be investigated in detail.

ACKNOWLEDGMENTS

This work was financially supported by DAE-SRC grant with sanction number: 2005/21/7-BRNS/2454.

[1]S. Ichimaru, Rev. Mod. Phys. **54**(4), 1017 (1982).
[2]P. K. Shukla and B. Eliasson, Rev. Mod. Phys. **81**, 25–44 (2009).
[3]G. E. Morfill and A. V. Ivlev, Rev. Mod. Phys. **81**(4), 1353–1404 (2009).
[4]A. Ng, P. Celliers, G. Xu, and A. Forsman, Phys. Rev. E **52**, 4299–4310 (1995).
[5]P. K. Shukla, A. A. Mamun, and D. A. Mendis, Phys. Rev. E **84**, 026405 (2011).
[6]T. Pohl, T. Pattard, and J. M. Rost, Phys. Rev. Lett. **92**, 155003 (2004).
[7]V. E. Fortov, I. T. Iakubov, and A. G. Khrapak, *Physics of Strongly Coupled Plasma*. (Clarendon, Oxford, 2006).
[8]H. Thomas, G. E. Morfill, V. Demmel, J. Goree, B. Feuerbacher, and D. Möhlmann, Phys. Rev. Lett. **73**, 652–655 (1994).
[9]J. H. Chu and I. Lin, Phys. Rev. Lett. **72**, 4009–4012 (1994).
[10]H. M. Thomas and G. E. Morfill, Nature **379**, 806–809 (1996).
[11]J. Frenkel, *Kinetic Theory Of Liquids* (Dover, 1955).
[12]P. K. Kaw and A. Sen, Phys. Plasmas **5**(10), 3552–3559 (1998).
[13]S. Nunomura, D. Samsonov, and J. Goree, Phys. Rev. Lett. **84**(22), 5141–5144 (2000).
[14]J. Pramanik, G. Prasad, A. Sen, and P. K. Kaw, Phys. Rev. Lett. **88**(17), 175001 (2002).
[15]P. G. Drazin, *Introduction to Hydrodynamic Stability* (Cambridge University Press, UK, 2002).
[16]S. Chandrasekhar, *Hydrodynamic and Hydromagnetic Stability* (Clarendon, Oxford, 1961).
[17]S. K. Tiwari, A. Das, P. Kaw, and A. Sen, Phys. Plasmas **19**, 023703 (2012).
[18]S. K. Tiwari, A. Das, P. Kaw, and A. Sen, Phys. Plasmas **19**, 013706 (2012).
[19]S. Ichimaru, H. Iyetomi, and S. Tanaka, Phys. Rep. **149**(2–3), 91–205 (1987).
[20]S. M. Murillo, High Energy Density Phys. **4**(1–2), 49–57 (2008).
[21]A. Groisman and V. Steinberg, Nature **405**(6782), 53–5 (2000).
[22]J. P. Boris, A. M. Landsberg, E. S. Oran, and J. H. Gardner, LCPFCT—A flux-corrected transport algorithm for solving generalized continuity equations. Technical Report NRL Memorandum Report 93-7192, Naval Research Laboratory, 1993.